Surface measurements of aerosol properties over northwest China during ARM China 2008 deployment

Xin Wang,[1] Jiangping Huang,[1] Rudong Zhang,[1] Bin Chen,[1] and Jianrong Bi[1]

Received 29 October 2009; revised 15 June 2010; accepted 27 July 2010; published 4 November 2010.

[1] To improve understanding and capture the direct evidence of the impact of dust aerosol on climate, the 2008 China-U.S. joint field campaigns are conducted. Three sites are involved this campaign, including one permanent site (Semi-Arid Climate and Environment Observatory of Lanzhou University (SACOL)) (located in Yuzhong, 35.95°N, 104.1°E), one SACOL's Mobile Facility (SMF) (deployed in Jintai, 37.57°N, 104.23°E), and the U.S. Department of Energy Atmospheric Radiation Measurements (ARM) Ancillary Facility (AAF mobile laboratories, SMART-COMMIT) (deployed in Zhangye, 39.08°N, 100.27°E). This paper presents the results of direct measurement analysis of the dust plume transport case. During the dust plume period, the OMI AI data and air mass back trajectory model (HYSPLIT) clearly illustrated that the air mass originated from the Taklamakan desert and Inner Mongolia Gobi desert. The daily averaged concentrations of PM_{10} were about 0.2 ± 0.03 mg/m^3 at SACOL and Zhangye, but during the dust plume the mass concentration of dust aerosol were 0.98 mg/m^3 at Zhangye and 0.52 mg/m^3 at SACOL. The black carbon (BC) value reached its high peak during the dust plume. However, the concentration of BC was not only fluctuated with the dust plume, but also affected by the local air pollutants. When the dust plume occurred, the multiwavelength aerosol optical depth can be raised to ~2, ~1.5 times as high as that during the non dust plume period, and the number (mass) distribution during the dust plume showed the aerosol types considered correspond to urban/industrial aerosols, coarse mode particles. The meteorological analysis indicated that these polluted layers are not only transported from their sources, but also include the local sources.

Citation: Wang, X., J. Huang, R. Zhang, B. Chen, and J. Bi (2010), Surface measurements of aerosol properties over northwest China during ARM China 2008 deployment, *J. Geophys. Res.*, *115*, D00K27, doi:10.1029/2009JD013467.

1. Introduction

[2] Air pollution in East Asia includes particles from large and growing sources of dust aerosols and other atmospheric pollutants [*Jaffe et al.*, 1999; *Zhang et al.*, 2010]. In particular, air pollutant emissions have increased rapidly in China since the 1980s as a consequence of industrial development, economic growth, and large-scale rural-to-urban migration. This has led to various air pollution problems [*Wang et al.*, 2004; *Li et al.*, 2010]. Dust aerosols emitted in China impact more than the local environment and human health, as they appear to have an unusually broad range of influence [*R. J. Zhang et al.*, 2003, 2005; *Huang et al.*, 2006a]. Recent studies detected emissions from East Asia as far downwind as the western Pacific [*Gong et al.*, 2003; *Huang et al.*, 2008a]. Extensive ground-based and airborne-based measurement campaigns have examined the transport of air masses from land regions to the Pacific, including the Asia-Pacific Regional Aerosol Characterization Experiment (ACE-Asia) [*Conant et al.*, 2003] and the East Asian Study of Tropospheric Aerosols: An International Experiment (EAST-AIRE) [*Z. Li et al.*, 2007a]. The impact of the long-range transport of the dust plume and air pollutants from their continental sources over dust source regions is one of the outstanding problems in regional and global climate change research [*Streets et al.*, 2001; *Lelieveld et al.*, 2001; *Dickerson et al.*, 2002; *Nakajima et al.*, 2003; *Li*, 2004; *Xia et al.*, 2004; *Qian et al.*, 2009]. Dust mixed with anthropogenic aerosols creates a brownish haze which absorbs and scatters sunlight and reduces solar illumination at the surface [*Ramanathan et al.*, 2001], causing the "global dimming" effect. Dust outbreaks can affect the radiation balance in the atmosphere over the nearby Taklamakan Desert [*Arimoto et al.*, 2004; *Xia et al.*, 2007; *Lee et al.*, 2010]. Dust plumes can also accumulate over the Tibetan Plateau where they both absorb and reflect solar radiation [*Wang et al.*, 1999; *Huang et al.*, 2007]. *Huang et al.* [2006b] investigated the interactions of desert dust with clouds can have substantial climatic impacts due to the large spatial and temporal extent of desert dust in the atmosphere. Dust plumes mainly occur during springtime responses of

[1]Key Laboratory for Semi-Arid Climate Change of the Ministry of Education, College of Atmospheric Sciences, Lanzhou University, Lanzhou, China.

0148-0227/10/2009JD013467

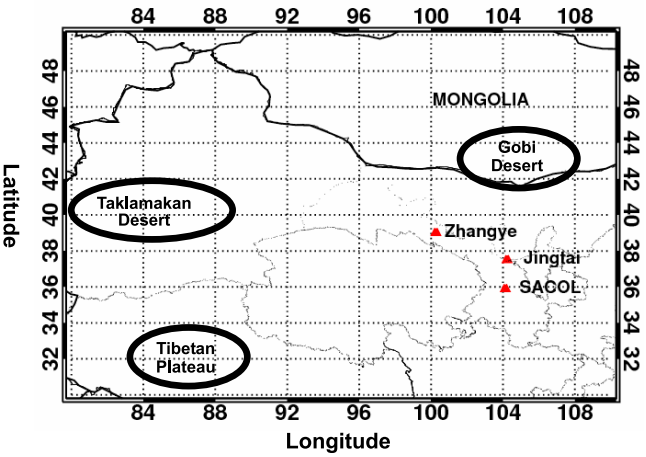

Figure 1. Location of Lanzhou University Semi-Arid Climate and Environment Observatory (SACOL).

climate change to the aerosol depend strongly on its optical and physical properties [*Ge et al.*, 2010], especially March and April [*Littmann*, 1991]. Several studies have reported that transport across the Pacific from Asia to North America is sufficiently fast to contribute significantly to the atmospheric loading of black carbon (BC) [*VanCuren et al.*, 2005; *Gu et al.*, 2010] and carbon monoxide [*de Gouw et al.*, 2004; *Jaffe et al.*, 2005]. Long-range transport of air pollution over the Pacific Ocean has been studied extensively by examining surface data along the west coast of North America [*VanCuren et al.*, 2005; *Jaffe et al.*, 2005, *Huang et al.*, 2008a], by airborne campaigns such as the Intercontinental Transport and Chemical Transformation of Anthropogenic Pollution (ITCT) [*Heald et al.*, 2005; *Brock et al.*, 2004] and Transport and Chemical Evolution over the Pacific (TRACE-P) [*M. Zhang et al.*, 2003] projects, by examining satellite data [*Husar et al.*, 2001], and by the Indian Ocean Experiment (INDOEX) campaign [*Verma et al.*, 2005]. The direct radiative forcing of dust and air pollutants were also studied during the ACE-Asia project [*Kim et al.*, 2005], which compiled a large number of observations of polluted air masses leaving the Asian continent [*Huebert et al.*, 2003]. While the ACE-Asia project generally was not able to sample regions of largest dust concentration, the study revealed that dust in the free troposphere contained less evidence of anthropogenic pollution than dust in the marine boundary layer. *Gong et al.* [2004] estimated that depending on the degree of desertification, newly formed deserts covered 15% to 19% of the original desert area and would generate from 10% to 40% more dust storms under the same meteorological conditions as for spring 2001. Studies of dust deposition indicated potential distributions on global scales [*Prospero*, 1996, 1999]. Large-scale sources include the African Sahara and eastern Asia [*Huebert et al.*, 2003]. Another international, multiplatform campaign, the Mediterranean Intensive Oxidant Study (MINOS) campaign, measured the long-range transport of air pollution and dust aerosols from Southeast Asia and Europe toward the Mediterranean basin during August 2001. Ground, airborne, and satellite-based measurements of suites of chemical compounds combined with backward trajectory analyses have been used over the past 2 decades to document approximately 20 plumes of air pollution from Asia reaching the west coast of North America [*VanCuren and Cahill*, 2002].

[3] Direct measurements of dust aerosols close to source regions are still insufficient for understanding the air pollution problem in East Asia. To characterize the emission, transport, and removal of atmospheric pollutants from East Asia, a China 2008 deployment was conducted from late April to May 2008, focusing on direct measurements of Asian dust and pollution transport. A plume was followed from northern China (the Taklamakan and Gobi deserts) to the eastern Pacific and into North America. These measurements must include basic physical and chemical characterization of the aerosols, particularly the BC and dust compositions, the albedo of the dust pollution layer (measured from above plumes, which can have top heights as high as 15 km), and the transmission of solar radiation through the layer to determine the magnitude of dimming across the Pacific Ocean.

[4] The China 2008 experiment took place in Lanzhou, China, from late April to May 2008. The primary component affecting aerosol light absorption is BC, which efficiently absorbs light at all wavelengths. Black carbon is a byproduct of incomplete combustion and a constituent of soot, and numerous modeling studies have demonstrated its importance in regional climate change [*Chung et al.*, 2002; *Menon et al.*, 2002; *Ramanathan et al.*, 2005]. Three sites were involved in the China 2008 campaign, including one permanent site (the Semi-Arid Climate and Environment Observatory of Lanzhou University, SACOL, located in Yuzhong, 35.95°N, 104.1°E), a mobile facility of SACOL (deployed in Jintai, 37.57°N, 104.23°E), and the U.S. Department of Energy Atmospheric Radiation Measurements, Ancillary Facility (AAF mobile laboratory, SMART-COMMIT, deployed in Zhangye, 39.08°N, 100.27°E).

[5] This paper presents detailed emission information obtained from measurements made in Lanzhou during the China-U.S. 2008 deployment (Z. Li et al., Overview of the East Asian Study of Tropospheric Aerosols and Impact on Regional Climate (EAST-AIRC), manuscript in preparation, 2010), with the aim of better understanding regional emission sources and the characteristics of air pollution over northwestern China, including dust aerosol and BC pollution. On the basis of statistical analysis, possible signatures of dust plumes transported over long ranges from remote emission sources were also identified.

2. Observations

2.1. Measurement Sites

[6] The SACOL observatory is a facility built in the Loess Plateau area of northwestern China (Figure 1) [*Huang et al.*, 2008b], very close to the geometric center of mainland China. The observatory is established to provide data for quantitative estimations of the aerosol forcing effect and assessment of human impacts on regional climate. Prior to establishment of SACOL, there had been no such kind of observatory in the northwest region, the largest arid/semiarid zone in China. Research using SACOL data focuses on investigating natural and anthropological pollution on the regional climate scale. In addition, observations from SACOL can indicate the mechanisms of climatic and environmental changes in China. Severe water shortages and rapid population increases, for example, can

Table 1. Instrumentation Operating at SACOL

Parameter	Instrument Type and Manufacturer	Accuracy
Aerosol spectral optical depth	CE318N-VPS8, CIMEL Sun photometer (AOD at 340, 380, 440, 670, 870, 936, 1020nm), AERNET	~ ±2%
Aerosol light absorption properties	Aethalometer (Model AE-31, Magee Sci.) at seven wavelengths (370, 470, 520, 590, 660, 880 and 950nm)	0.1 ug/m^3
Aerosol scattering coefficient	Integrating Nephelometers (M9003, ECOTECH) (450, 520 and 700nm)	0.5 Mm^{-1}
PM_{10}	Ambient Particulate Monitor (RP1400a, Thermo)	0.1 ug/m^3

cause substantial anthropological impacts on climate and the environment via land use changes and greenhouse gas emission.

[7] To characterize the emission, transport, and removal of atmospheric pollutants from East Asia, the China-U.S. 2008 project was performed from late April to May 2008 (Z. Li et al., manuscript in preparation, 2010), with a specific focus on direct measurements of Asian dust and pollution transport. A plume from northern China (the Taklamakan and Gobi deserts) was tracked over the eastern Pacific and into North America. Such measurements are crucial to understand how dust and pollution plumes are transported from Taklamakan desert region to remote region.

2.2. Instruments

[8] Table 1 lists the aerosol instrumentation at the SACOL site. The data reported here are from the following instruments. The mass concentration of particulate matter 10 μm or less (PM_{10}) was measured continuously by an R&P 1400a analyzer using the principle of tapered element oscillating microbalance (TEOM) with an appropriate sample inlet. The collector is operated at 50°C to dry the aerosol and a flow rate of 16.7 L/M. Such heating is known to produce a slight loss of volatile compounds. A seven-wavelength aethalometer™ (Magee Scientific model AE-31) took measurements at 5 min intervals. This device is previously described by *Fialho et al.* [2005]. An integrating nephelometer (TSI Model 3563) is employed to measure aerosol scattering coefficients (bsp) at three wavelengths. For an averaging interval of 5 min, the detection limits of the instrument at 450, 550, and 700 nm were 0.44×10^{-6} m^{-1}, 0.17×10^{-6} m^{-1}, and 0.26×10^{-6} m^{-1}, respectively (signal-to-noise ratio S:N = 2:1 [*Anderson et al.*, 1996]). Time series of AERONET (version 2, level 1.5) aerosol optical depth (AOD) at 500 nm wavelength, fine mode and coarse mode AOD, and the fine mode fraction and multiwavelength AOD over SACOL were obtained during the dust plume from NASA Goddard Space Flight Center (GSFC) (http://aeronet.gsfc.nasa.gov). Daily zonal wind profiles over SACOL were taken from National Centers for Environmental Prediction-National Center for Atmospheric Research (NCEP-NCAR) reanalysis data (http://www.cdc.noaa.gov/) at 2.5 × 2.5 degree resolution (Figure 3). We used National Oceanic and Atmospheric Administration (NOAA) Air Resources Laboratory (ARL) Hybrid Single-Particle Lagrangian Integrated Trajectory Model (HYSPLIT, http://www.arl.noaa.gov) back trajectories to locate the source region of the dust plume and capture the vertical movement of the air mass from its source to the receptor (SACOL) at three different heights that affected SACOL during 28 April to 3 May 2008.

2.3. Satellite Data

[9] Daily data sets of aerosol index (AI) values from the Ozone Monitoring Instrument (OMI) of the Aura Satellite covering the study area were analyzed to study the variation in atmospheric aerosol loading. We used AI data from the Earth Observing System (EOS) Aura spacecraft, which was launched in July 2004 [*Ahmad et al.*, 2003]. The OMI AI archive has been shown to be a useful qualitative indicator of the presence of absorbing aerosols [*Duncan et al.*, 2003]. The OMI AI can differentiate very well between absorbing and nonabsorbing aerosols by providing a measure of the absorption of UV radiation by smoke and desert dust [*Torres et al.*, 1998]. The absorbing AI is defined as the difference between the measured (including aerosol effects) spectral contrast at 360 and 331 nm wavelength radiances and the contrast calculated from radiative transfer theory for a pure molecular (Rayleigh scattering) atmosphere.

[10] The AI is defined mathematically as

$$\mathrm{AI} = -100[\log_{10}(\mathrm{I}_{360}/\mathrm{I}_{331})\mathrm{meas} - \log_{10}(\mathrm{I}_{360}/\mathrm{I}_{331})\mathrm{calc}]$$

Because the I_{360} calculation uses reflectivities derived from the I_{331} measurements, the AI definition essentially simplifies to

$$\mathrm{AI} = 100\log_{10}(\mathrm{I}_{360\_\mathrm{meas}}/\mathrm{I}_{360\_\mathrm{calc}})$$

The CALIPSO Cloud-Aerosol Lidar with Orthogonal Polarization (CALIOP) instrument measures vertical profiles of elastic backscatter at 532 and 1064 nm near nadir during both day and night phases of the orbit. The primary products are three calibrated and geolocated lidar profiles of 532 and 1064 nm total attenuated backscatters and a 532 nm depolarization ratio, which is computed from the two polarization components of the attenuated backscatter. The CALIPSO level 2 data products (version 1.10) contain the cloud and aerosol layer and column properties. Level 1B data are first averaged into 5 km cloud layer products that are used to screen out cloudy profiles [*D. Liu et al.*, 2008].

[11] Dust aerosols can be identified in a given altitude range of a lidar profile using the volume depolarization ratio (VDR), defined as the ratio of the perpendicular to parallel components of received lidar signals (including both particulate and molecular scattering) at 532 nm. The depolarization ratio is normally used as an indicator to separate dust from other aerosol types [*Murayama et al.*, 2001].

3. Analysis of Results

[12] A strong dust plume occurred on 2 May 2008, during the China 2008 campaign. To identify the plume, we mapped the daily mean OMI-retrieved AI from 28 April to 3 May 2008. Figure 2 shows a large plume of dust (OMI image)

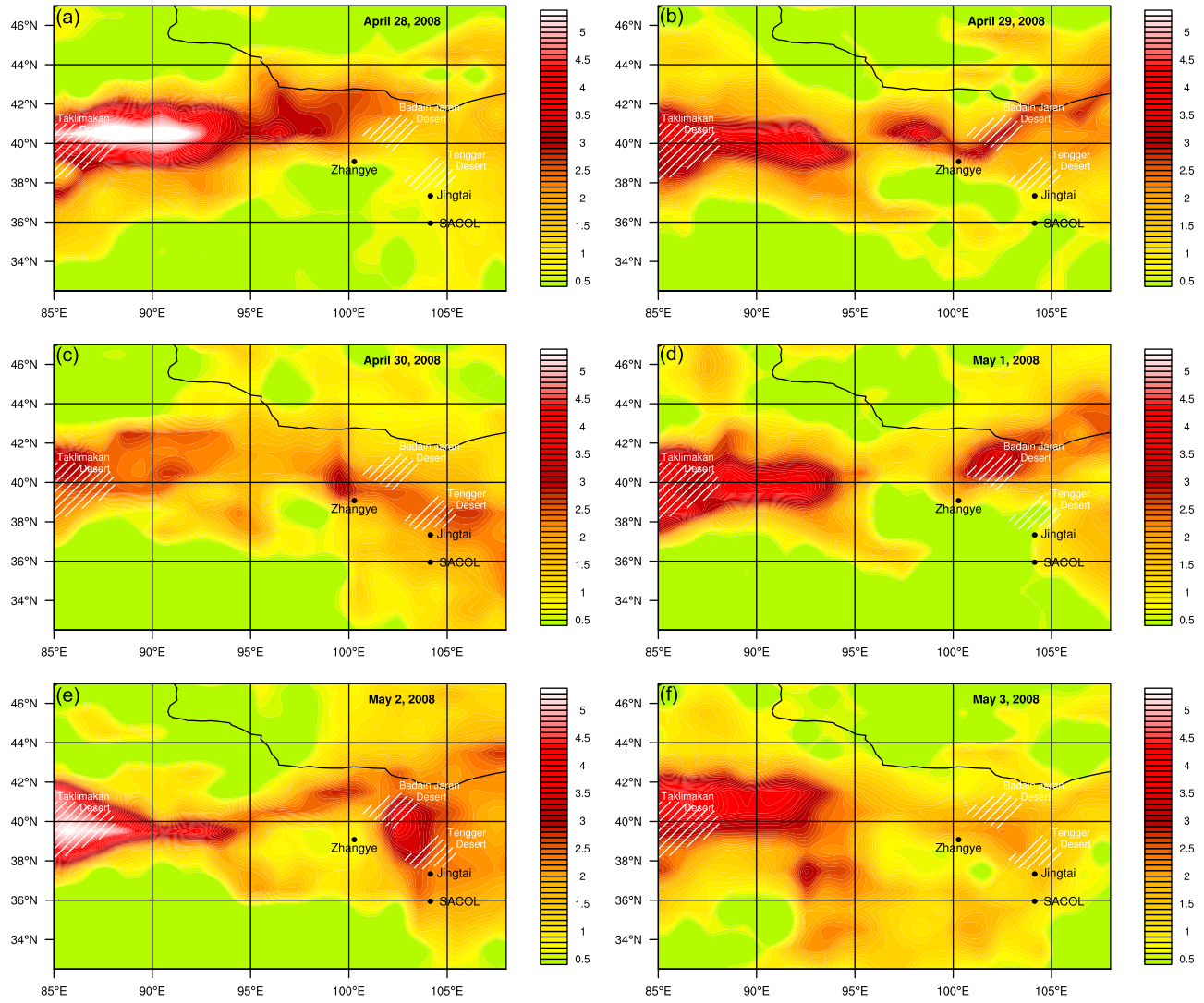

Figure 2. OMI daily aerosol index during the evolution of a dust plume at SACOL for (a) 28 April 2008, (b) 29 April 2008, (c) 30 April 2008, (d) 1 May 2008, (e) 2 May 2008, and (f) 3 May 2008.

over northwestern China from 28 April to 3 May 2008. The AI reached large values (more than five) in the center of the Taklamakan Desert, suggesting higher concentration of absorbing aerosols over that region during this large dust plume. These plots clearly illustrated a dust plume over the Gobi and Taklamakan deserts and its transport eastward. *Wang et al.* [2008] analyzed surface observations from 701 meteorological stations over the period 1960 to 2004 and found that the Taklamakan Desert in western China and the Gobi Desert in Inner Mongolia were the two major sources of dust storms in China. In all, 800 Tg of dust from China was estimated to be injected into the atmosphere annually, this may be as much as half of the global production of dust [*Zhang et al.*, 1997]. The OMI AI (Figure 2) confirmed the dominance of Taklamakan Desert sources. A large area stretching from this region had relatively high AI values during this dust plume, which exceeded 5 in the center of the Taklamakan Desert region on 28 April. The dust plume shows maximum values of more than 3 from 29 April to 1 May, moved to the east over SACOL on 2 May, and then moved to northeast China. Figure 2f showed this large dust plume moved toward the Badan Jaran Desert and affected SACOL, Jingtai, and Zhangye on 2 May 2008.

[13] Figure 3 shows four-times-daily NCEP reanalysis pressure level geopotential heights at 500 hPa. A synoptic low-pressure system that developed in northwestern China created high wind speeds at 500 hPa over an extended region that included north central China at 00:00 UTC 2 May 2008 (Figure 3a). In the following hours, the cyclone continued to propagate eastward when the dust plume was over SACOL. Wind subsequently came from the northwest with the low-pressure system and its accompanying cold front (Figures 3b to 3d), affecting SACOL, Jingtai, and Zhangye on 2 May 2008. This indicated that the dust plume was trapped by the low-pressure system and its accompanying cold front from northwest to west, which approached Xinjiang Province on 2 May 2008 and then continued westward. During this period, the instruments taking measurements over SACOL, Jingtai, and Zhangye were observing more signals from nearby emission sources, as wind speeds were relatively low and

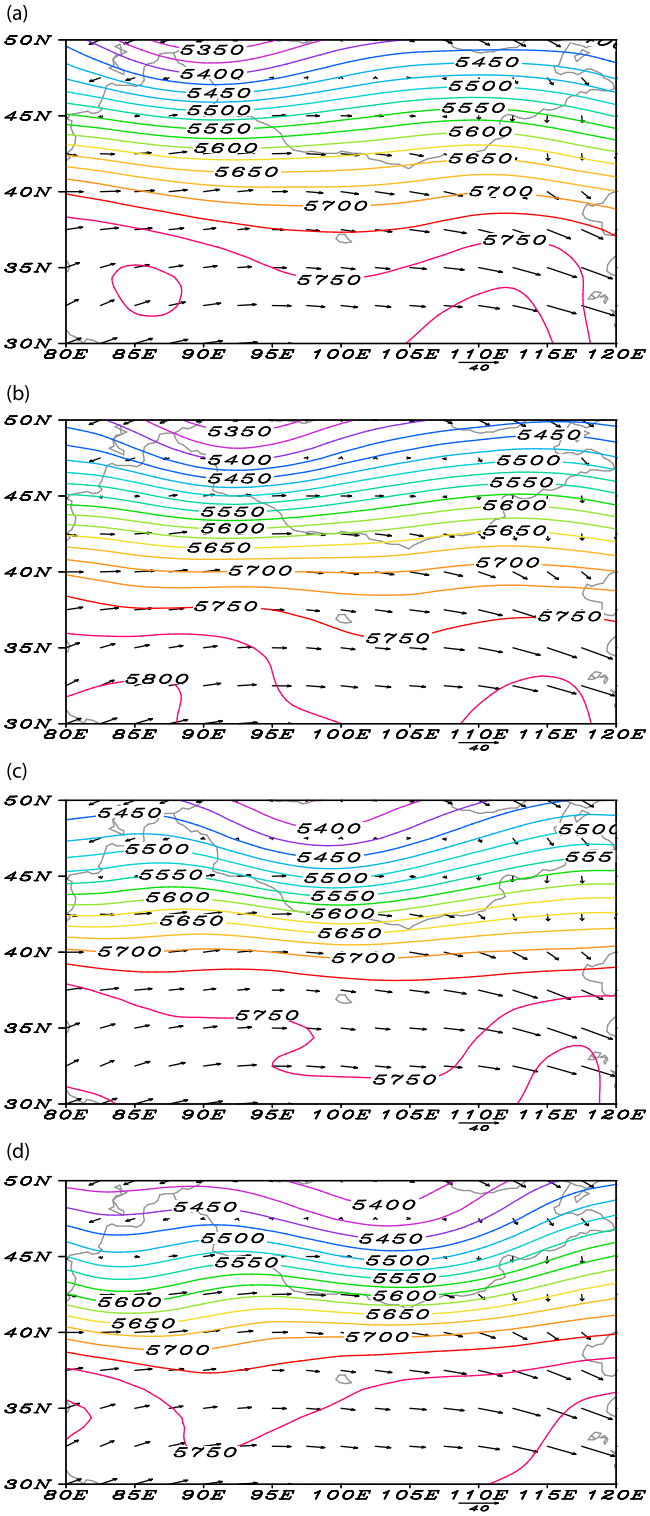

Figure 3. Geopotential height at 500 hPa level for (a) 0000 UTC, 2 May 2008, (b) 0600 UTC, 2 May 2008, (c) 1200 UTC, 2 May 2008 and (d) 1800 UTC, 2 May, 2008 based on NCEP/NCAR reanalysis data.

atmospheric mixing was relatively weak. The stronger mixing and higher wind speeds during the daytime helped to transport mixed plume from a larger region to SACOL. Data from different times during the dust plume could therefore be used to characterize the emission sources of different regions. *Sun et al.* [2001] suggested that dust plumes over the Taklamakan Desert were mainly associated with the western route of cold air outbreaks, which usually occurred due to easterly winds in the desert region. *Gong et al.* [2003] found that dust plumes were associated with prevailing meteorological conditions. *Ding et al.* [2005] arrived at the same conclusion using monthly meteorological data associated with dust events observed at 701 meteorological stations.

[14] We also used daily vertical profiles of zonal wind speed and vertical velocity omega from NCEP-NCAR reanalysis products. The daily mean vertical profiles of zonal wind speed and omega over SACOL, Jingtai, and Zhangye from 28 April to 3 May 2008 are shown in Figures 4a–4f. The wind velocity increased with height during the dust plume (negative zonal wind indicates a wind direction from east to west, while positive indicates the opposite). In both locations, the zonal wind velocity had two distinct regimes: that from 28 to 30 April (prior to the dust storm) and that from 1 to 3 May during the dust plume. Figures 4a, 4c, and 4e show the differences in wind velocity between the dust plume and non dust plume periods at different pressure levels. During the dust plume passage, average wind velocity nearly doubled compared to that prior to the dust plume at different pressure levels. Most of the time, wind speeds were low (in the range 5 to 30 m/s). Figures 4b, 4d, and 4f show the vertical velocity (omega in Pa/s) profile before and after the dust plume passed over SACOL, Jingtai, and Zhangye. Before this (28–30 April), omega was mostly positive (>0 Pa/s) from the surface to 100 hPa, indicating little or no upward movement of air. With the advent of the dust plume on 1 May (Figures 4d and 4f), omega showed a prominent negative value that was associated with the upward vertical motion of air. A strong shift toward negative values occurred at 400–850 hPa. Omega values were −0.07 Pa/s at SACOL and −0.15 Pa/s at Jingtai at 500 hPa on 1 May 2008. After the dust plume period, omega also showed a prominent negative value on 3 May 2008. During the dust plume period on 2 May 2008, omega was positive, indicating that the dust was floating. *Sun et al.* [2001] suggested that dust plumes over the Taklamakan Desert are mainly associated with the western route cold air outbreaks, which usually occur due to easterly winds in the desert region.

[15] To investigate the dust plumes, we used the HYSPLIT back-trajectory model (starting on 1 May 2008) to capture the transport path from the dust origins [*Draxler and Hess*, 1998] (http://www.arl.noaa.gov/ready/hysplit4.html). The HYSPLIT simulation suggested the air masses corresponding to the dust layers originated above the Taklamakan and Inner Mongolian Gobi deserts [*Huang et al.*, 2007]. Figure 5 clearly illustrates that the air mass came from two pathways above ground level (AGL) over SACOL, originating from the Taklamakan and Inner Mongolian Gobi deserts. The trajectory analysis also confirmed the uplift of dust-laden air masses at Jingtai, Zhangye, and SACOL at altitudes of 500, 1000, and 2000 m AGL, capturing the vertical movement of

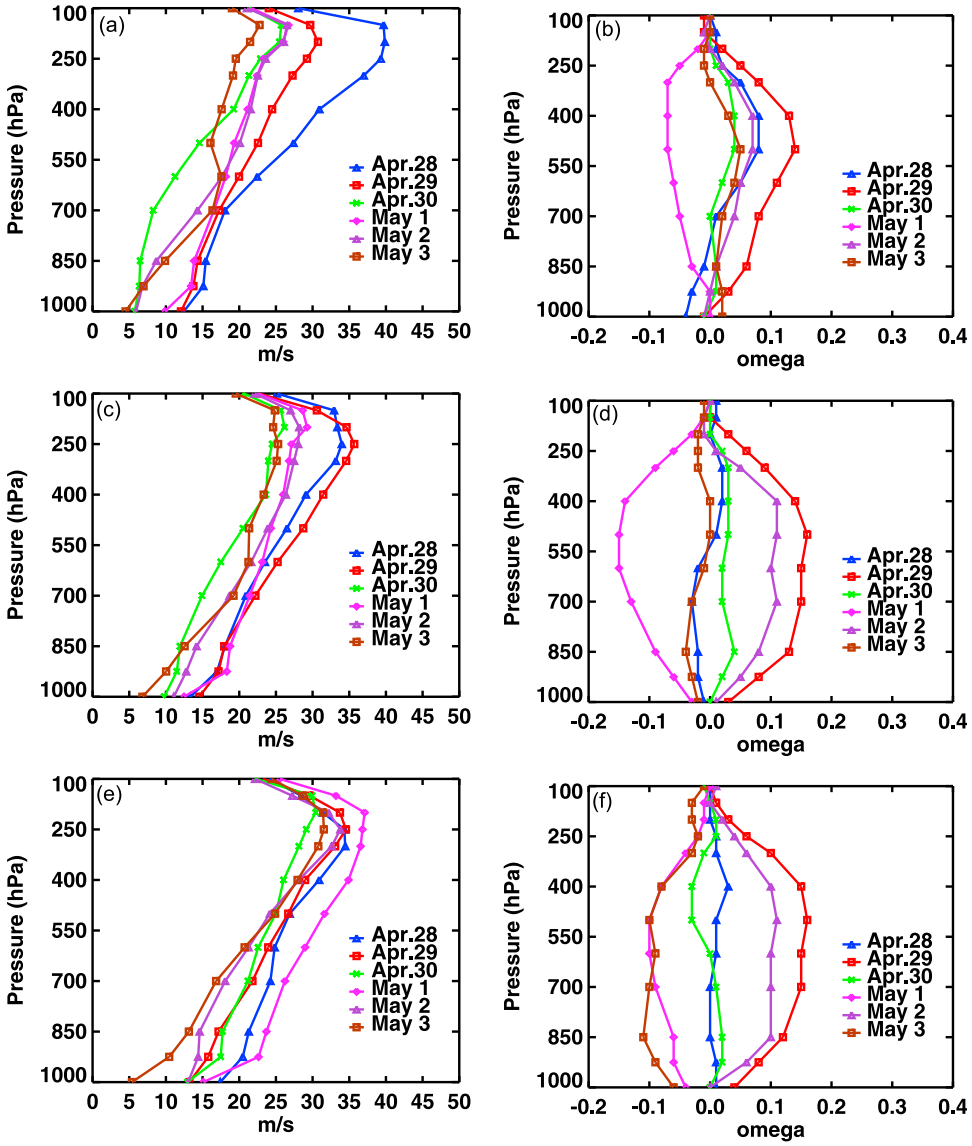

Figure 4. Daily vertical profile of zonal wind speed and Omega from NCEP reanalysis data over SACOL, Jingtai, and Zhangye from 28 April to 3 May 2008.

the dust storm from the source to the receptor. The HYSPLIT back trajectory for Jingtai (starting on 28 April 2008), Zhangye, and SACOL showed the source region of the dust plumes are Taklamakan desert and Gobi desert regions (Figure 5). Air mass trajectories originating from Jingtai at 15:00 (LST) were calculated back in time for 48 h. As shown in Figure 5a, the pathway of the dust air mass came from the west, originating from the Gobi Desert in Inner Mongolia. Figures 5b and 5c show two pathways from the Inner Mongolian Gobi Desert and Taklamakan Desert source regions, as shown in Figure 3. The transport of the dust plume was strongly related to the meteorological conditions at 500 hPa.

[16] CALIPSO observations taken during 6 nights (2–7 May) over China and the Pacific, and back trajectories illustrated the time evolution and transport of the dust during the event (Figure 6). The red lines represented 500–2000 m back trajectories produced by the HYSPLIT model. The 6 day back trajectories were initialized on 7 May in the western Pacific. They originate in central China and extend to the Taklamakan desert. The vertical images superimposed on the map show the CALIPSO 532 nm attenuated backscatter observations over the dust transport track. In these images, clouds appear as red, gray, or white and aerosols are shown in green, yellow, or orange [*Z. Liu et al.*, 2008; *Huang et al.*, 2010]. The images from the CALIPSO observations coupled with the back trajectory analysis in Figure 6 indicate that the dust originated over the Taklamakan on 2 May 2008 (or perhaps somewhat earlier). The nighttime CALIPSO observations in Figure 6 confirmed that the dust plume originated in the Taklamakan desert region.

[17] Figure 7 shows the heavy aerosol loadings associated with the dust plume at SACOL and Zhangye. Daily averaged PM_{10}, the aerosol scattering coefficient, and daily average concentrations of BC are also shown in Figure 7. On the basis of analyses of the variations in the aerosol scattering

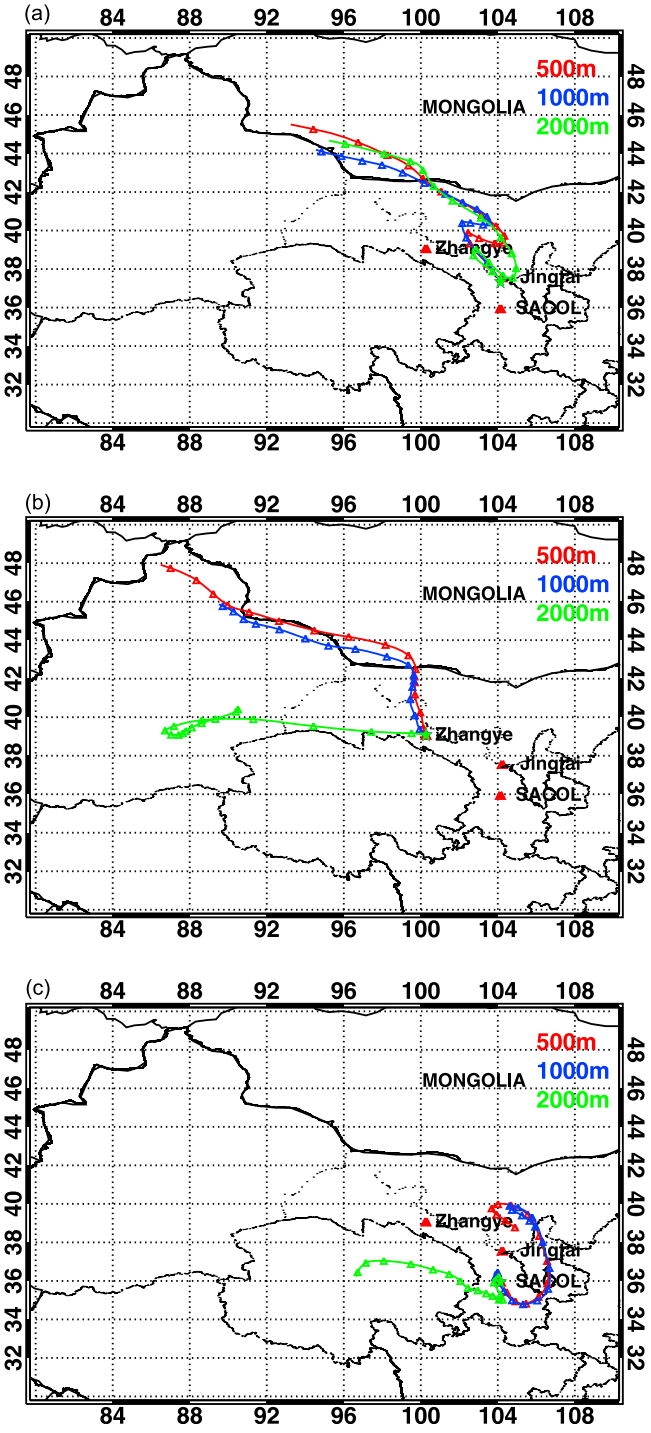

Figure 5. HYSPLIT air mass 2 day back trajectory of air parcels with initial position (starting 2 May, 15z) during a dust plume at three heights above ground level (AGL).

coefficient and PM_{10} concentration (Figure 7a), an inversion test of aerosol volume distributions was carried out with the measured aerosol spectral scattering coefficients at three wavelengths. The daily average concentrations of PM_{10} were 0.2 mg/m^3 at SACOL and Zhangye, but during the dust plume, the very high aerosol loadings had dust aerosol mass concentration of 0.98 mg/m^3 over Zhangye and 0.52 mg/m^3 over SACOL. Thus during the dust plume period, the mass concentration of dust aerosol was higher at Zhangye than at SACOL. The temporal variations of the scattering coefficient (Figure 7b) agreed well with the PM_{10} concentration. During the dust plume period, scattering coefficients reached 402.5 Mm^{-1} ($\pm 1\sigma$) at Zhangye and 187.75 Mm^{-1} ($\pm 1\sigma$) at SACOL, but during an intensive field campaign at Xianghe in 2005 at the same wavelength (550 nm) the scattering coefficient reached 940 Mm^{-1} ($\pm 1\sigma$) during the polluted period [*C. Li et al.*, 2007]. During this period of measurement, the average aerosol scattering coefficient, as measured by the nephelometer, was 95.51 Mm^{-1} ($\pm 1\sigma$) at Zhangye and 56.01 Mm^{-1} ($\pm 1\sigma$) at SACOL during the non dust plume period. The most prominent feature was that the average aerosol scattering coefficient at SACOL was less than that at Zhangye, as revealed in Figure 7b. The value of the scattering coefficients gradually increased following the increase in PM_{10} and peaking during the dust plume. The scattering coefficients gradually decreased after the dust plume. During the clean air period, the scattering coefficients were very low compared to during the air pollution conditions. The duration of the experiment was not long enough for a full-scale characterization of the seasonal changes in air pollution at SACOL. The daily average concentration of BC (Figure 7c) was measured using an AE-31 aethalometer to investigate the transport and evolution processes at the Loess Plateau during springtime. The average concentration of BC suggested it was closely related to the dust plume over northwestern China. There are two possible explanations for the slight BC decrease. One is seasonal changes in meteorological conditions. The other is seasonal changes in the intensities of the emission sources. Specifically, more biomass burning occurs in spring than from late spring to early fall. The in situ measurements reflected the aerosol composition after air had been transported substantial distances from the source region. The aerosol composition and size distribution depended critically on the air mass history. As shown, BC peaked during the dust plume. However, the variation showed that BC was affected by both the dust plume and local air pollutants. Hence the apparently high concentration of dust aerosol and low concentration of BC may have had different origins. The correlation coefficient between dust aerosol and BC was statistically significant at 1%. However, Figure 7 shows slight seasonal changes in May, the month of transition from late spring to early summer in northwestern China. The pronounced springtime maximum of PM_{10} at SACOL may reflect the effect of transport from East Asia in spring; note also the similarity with BC. The most obvious seasonal feature is the general decreasing trend of the PM_{10} and BC concentrations. The PM_{10} concentration at SACOL was even lower in May than in March and April during springtime [*Littmann*, 1991; *Zhou and Wang*, 2002].

[18] To better understand aerosol effects on climate and the environment, a number of studies have used ground-based aerosol Sun photometers to reveal the characteristics of aerosol optical properties over China [*Xia et al.*, 2005, 2006; *Z. Li et al.*, 2007b]. The AOD at a given wavelength is a standard parameter measured by Sun photometers such as those operating at AERONET sites [*Holben et al.*, 1998] (http://aeronet.gsfc.nasa.gov). The AOD represents the extinction of radiation at a given wavelength due to the

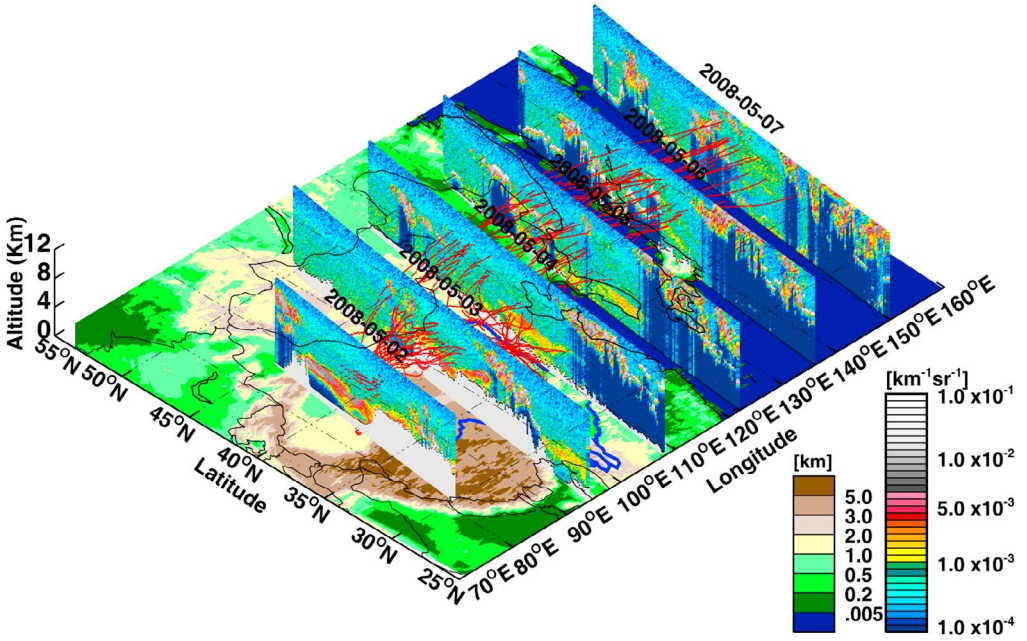

Figure 6. Illustration of the dust plume, which originated in the Taklamakan Desert on 2 May 2008 and was transported to the Sea of Japan. Red lines represent back trajectory analyses and show dust transport. Vertical images (curtain files) show the CALIPSO 532 nm total attenuated backscatter. The color scales on the left represent topographical elevation, and the color scales on the right represent 532 nm total attenuated backscatter.

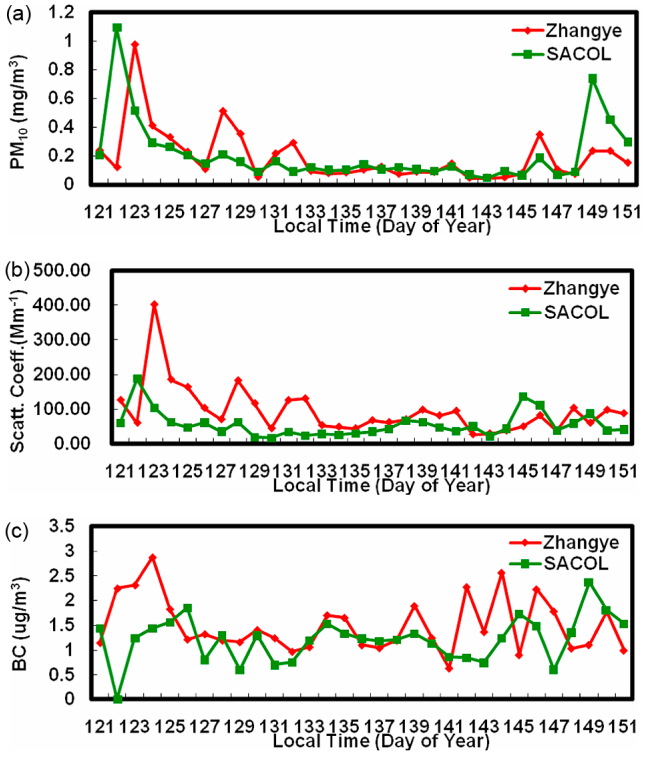

Figure 7. (a) Hourly averaged PM_{10}, and the hourly averaged concentrations of (b) aerosol scattering coefficient (450nm) and (c) BC observed over SACOL (green) and Zhangye (red) during 1–31 May 2008.

presence of atmospheric aerosols. The multiwavelength time series of AERONET AOD (Figure 8) also showed the arrival of dust plumes over SACOL on 2 May 2008. This was supported by a sharp increase in the multiwavelength AOD in AERONET data over SACOL. Information on the distribution of the Asian dust plume and the quantity of dust produced is needed to quantify the effects of dust on climate. During the dust plume, the multiwavelength AOD was much higher than the mean AOD in the non dust plume period. During the dust plume period at 15:00 (LST), the multiwavelength AOD was 1.5 to 2 times higher than in the non dust plume periods. This indicated that the dust plume was

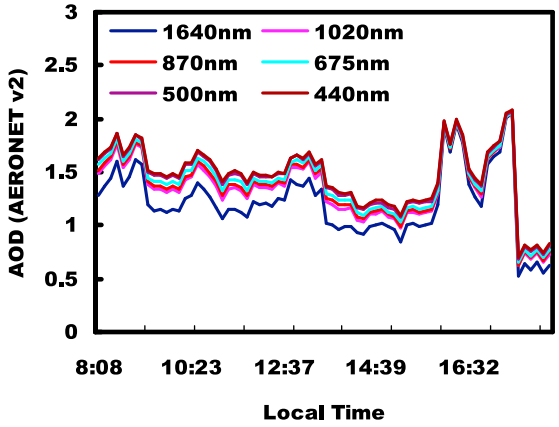

Figure 8. Wavelength dependency of multiwavelength AERONET AOD over SACOL is measured during 2 May 2008.

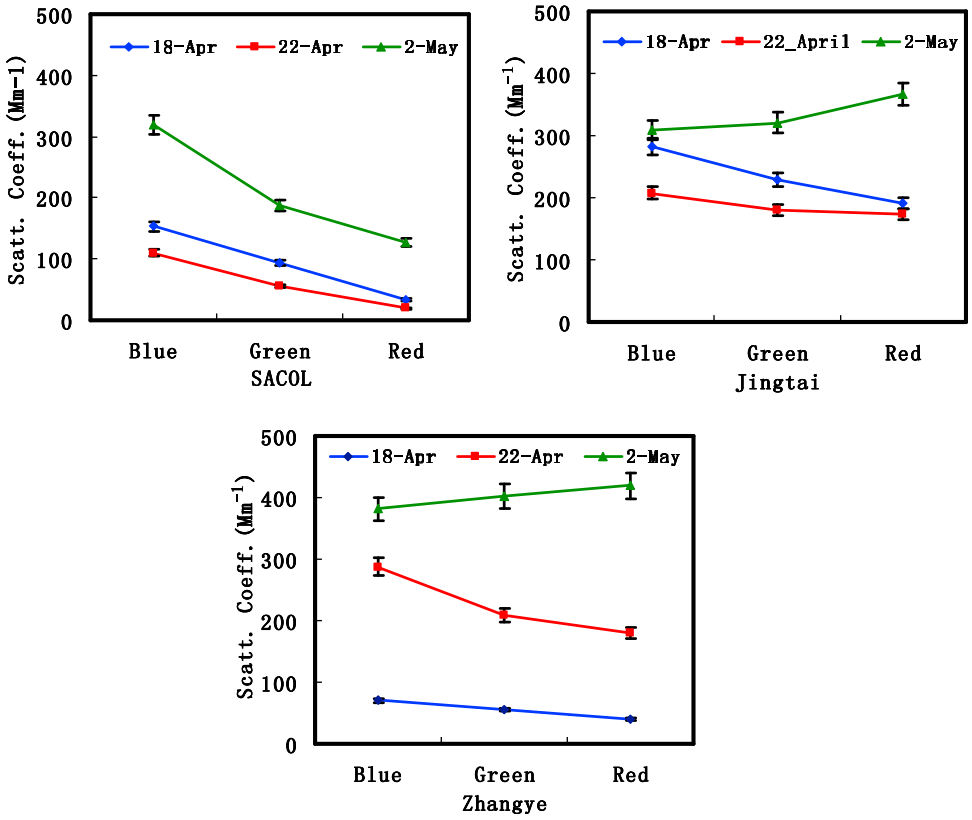

Figure 9. Daily averaged aerosol scattering coefficients (450 nm, 520 nm, 700 nm) observed at SACOL, Jingtai, and Zhangye before the non dust plume period (18 April and 22 April 2008) and during the dust plume on 2 May 2008. Error bars are 95% confidence limits of the mean values.

transported a long distance from its source and had a large influence on air quality in the study area. The observed dust plume was relatively intense and extensive, impacting a large area of northwestern China [*M. Zhang et al.*, 2003]. For comparison, high aerosol loading prevails at Xianghe year-round, with annual mean AOD of 0.82 [*Z. Li et al.*, 2006, 2007c].

[19] The nephelometer data required application of a correction routine to compensate for truncation errors and nonideality in the instrument geometry [*Anderson and Ogren*, 1998]. The correction factors were derived using the multiple wavelengths of the nephelometer to derive the Angstrom coefficient, which was then applied to a correction algorithm. Figure 9 shows the daily average aerosol scattering coefficients (450, 550, 700 nm) observed at SACOL, Jingtai, and Zhangye before (18 and 22 April 2008) and during (2 May 2008) the dust plume period. The error bars denote the 95% confidence limits of the mean values. The data were separated into average values for each wavelength during the dust and non dust plume periods. Error bars represent the 95% confidence limit of the average for each monsoon period. The dust plume period showed significant increases over SACOL, Jingtai, and Zhangye for scattering at all wavelengths. As shown in Figure 9, the scattering coefficients were 319, 188, and 127 Mm^{-1} for the dust plume period at SACOL for the three wavelengths of 450, 550, and 700 nm, respectively. For the same three wavelengths, values were 381, 402 and 419 Mm^{-1} at Zhangye and 308, 327, and 367 Mm^{-1} at Jingtai, respectively. The averaged values of the scattering coefficients at 520 nm were 94, 55, and 227 Mm^{-1} at SACOL, Zhangye, and Jingtai, respectively, during the non dust period on 18 April 2008; likewise, the average scattering coefficients were 56, 180, and 208 Mm^{-1} at those sites for the air pollutant period on 22 April 2008. For comparison, previous measurements during the dry monsoon as part of the INDOEX campaign found average scattering coefficients (at 70% relative humidity) of approximately 80 Mm^{-1} [*Eldering et al.*, 2002] and 28.8 Mm^{-1} at the Maldives Climate Observatory (Hanimaadhoo) [*Corrigan et al.*, 2006]. The lower scattering values during the non dust plume period were most likely due to submicron aerosols (D < 1 um) rather than PM_{10} (D < 10um). The large increase in absorption clearly indicated the arrival of polluted air from the Indian subcontinent at the Maldives because the only substantial source of broadband-absorbing particles is combustion processes. An increase in scattering might be attributable to a dust plume, but probably not at the consistent levels observed before 2 May 2008 over northwestern China at SACOL, Jingtai, and Zhangye.

[20] By combining the size distributions from aerodynamic particle sizer (APS) data, we obtained the total aerosol size and mass concentration information. In addition, the total mass of aerosols was retrieved directly from mass measurements using Teflon filters of PM_{10} size. Both the calculated aerosol size derived from the size distributions and the measured filter mass are plotted in Figure 10. The transition between 18 and 22 April and 2 May 2008 is also seen in Figure 10, but this change was not as significant as in the total particle concentration and submicron aerosol size dis-

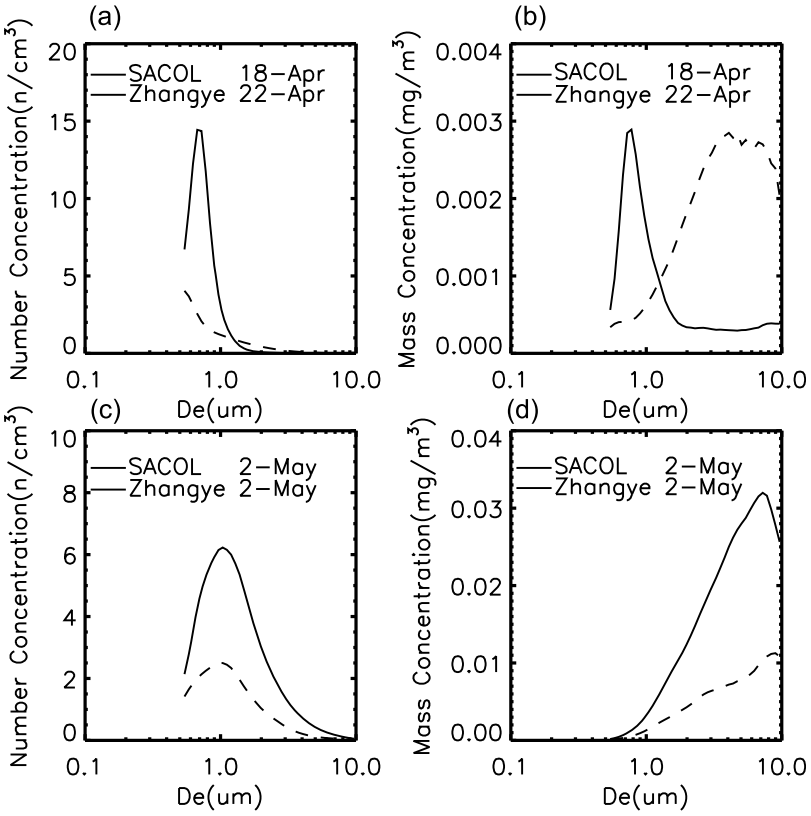

Figure 10. Daily averaged aerosol mass concentration and number size concentration against aerosol diameter over SACOL and Zhangye during the dust plume and non dust plume period. De denotes particle diameter.

tribution. This was mostly likely a result of the aerosol size being dominated by particles such as BC from local sources. Figure 10 shows the daily average aerosol mass and number concentrations against the aerosol diameter at SACOL and Zhangye during the dust plume and non dust plume periods. Using this detailed emissions inventory, we characterized the emissions from the dust plume in Figure 10. The most prominent feature of the air pollution at SACOL, as shown in Figure 10a, was the larger number concentration at SACOL than at Zhangye. There was a very close relationship between the number concentrations at SACOL and Zhangye during the non dust and dust plume periods. The number concentration of PM_{10} gradually increased in the range of 0.5–1 um, reaching a maximum value of 15 #/cm^3. It then decreased in the range > 1 um at SACOL during the non dust plume period. At Zhangye, the number concentration decreased gradually in the range of 0.5–10 um. Compared with the dust plume period, the diameter (De) of PM_{10} during the dust plume was larger than that during the non dust plume period. During the dust plume, De in the range > 1 um was larger than in the non dust plume period (Figure 10c). The concentration of PM_{10} was also much higher during the dust plume period than in the non dust plume period, and bsp agreed closely with PM_{10}. Figures 10b and 10d showed the mass concentration of PM_{10} during different weather conditions at SACOL and Zhangye. The mass concentration of PM_{10} had one peak during the non dust plume period. This indicated both fine and coarse mode aerosol particles occurred over SACOL. The mean mass concentration of PM_{10} for the rural background site before the dust plume arrived at SACOL and during the dust plume varied within a rather narrow range. The highest mass concentrations of PM_{10} were 0.03 and 0.01 mg/m3 at SACOL and Zhangye, respectively.

[21] Figure 11 shows the aerosol number distributions in the range 0.5 μm $\leq$ Dp [particle diameter] $\leq$ 20 μm observed at SACOL and Zhangye by the APS on 2 May 2008. In Figure 11, the aerosol types considered correspond to urban/industrial aerosols, coarse mode particles, and clean maritime conditions. We found three evident features with the number distributions at SACOL and Zhangye. First, accumulation mode particles increased at SACOL, with a maximum size distribution around 2–6 um in the morning during the dust plume, and decreased at Zhangye. Figure 11a shows that a larger number distribution of more than 10 #/cm^3 for particles around 0.5–1 um at SACOL during 2:00–8:00 (LST). During the dust plume, the fine and coarse mode particles decreased and floating dust was observed in the area. Second, the aerosol number concentration at SACOL had a second peak after 22:00 caused by frequent outbreaks of local pollutants. The local strong wind was most favorable for the occurrence of urban/industrial aerosols. The accumulation mode particles were enhanced with a maximum number concentration of particles approximately 0.3–0.4 mm in radius. This shift to larger particle size could have induced a larger AOD because the larger particles in the accumulation mode were more efficient at aerosol scattering. Atmospheric particles between 0.1 and 1.0 mm diameter scatter light most efficiently. Third, a distinct increase of both accumulation mode (a peak near

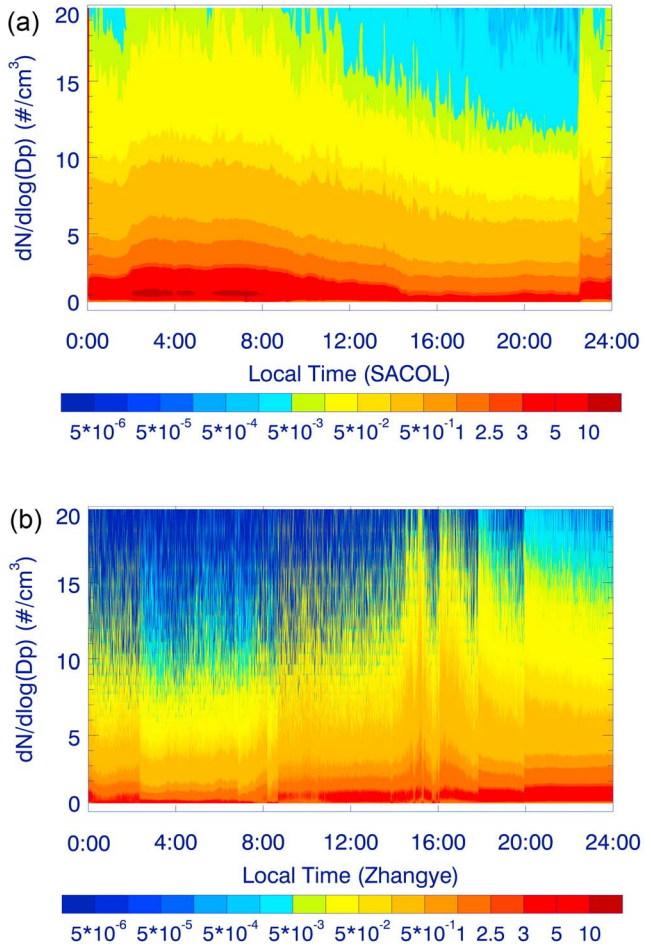

Figure 11. Time series of aerosol size distribution collected with a TSI APS measurements (0.5 um $\leqq$ De $\leqq$ 20 um) during 2 May 2008 at SACOL and Zhangye. De denotes particle diameter.

0.2 mm) and coarse mode aerosols (a peak around 4 mm at SACOL) occurred during the dust plume. Another feature seen in Figure 11b was that the coarse mode concentration during the dust plume was larger than that during the non dust plume period. Figure 11b shows all of the seasons exhibited obvious bimodal aerosol number distributions at Zhangye, due to fine and coarse mode particles. The number distribution relative maximum was evident at Dp ~ 0.6 μm, indicating possible shifting between the fine and coarse modes. This high value of the number distribution in the coarse mode may be related to the dust aerosols, which can produce large amounts of coarse mode particles. For comparison, *Zhang et al.* [2008] reported that, during the dust storm, the number concentration of coarse particles was 6.3 times larger than in the non dust storm period, but the number concentration of fine particles was only 1.3 times larger. This was because dust plumes and anthropogenic aerosols tended to be in the fine fractions.

4. Conclusions and Discussion

[22] Over northwestern China, dust aerosols have important effects on the atmospheric environment and climate in spring. In this study, the large dust plumes are examined. This plume caused by a low pressure over northeast Xinjiang Province on 2 May, which created strong winds at 500 hPa that bore high-density dust aloft over an extended desert region including northwestern China and then affected SACOL, Jingtai, and Zhangye. A 2 day back-trajectory projection by the HYSPLIT model (starting on 1 May 2008) showed the air mass came from two pathways at different levels from source regions in the Taklamakan and Inner Mongolian Gobi deserts. OMI AI reached large values (more than five) in the center of the Taklamakan Desert, suggesting higher concentration of absorbing aerosols over that region during this large dust plume. The nighttime CALIPSO observations confirm that the dust event originated from the Taklamakan desert region.

[23] During the dust plume period, in situ mass concentration of dust aerosols was higher at Zhangye than at SACOL, with scattering coefficients of 402.5 Mm^{-1} ($\pm 1\sigma$) and 187.75 Mm^{-1} ($\pm 1\sigma$), respectively. After the dust plume passed, the scattering coefficients tended to decrease gradually. The multiwavelength AERONET AOD showed the arrival of the dust plume over SACOL on 2 May 2008, which was supported by a sharp increase in the multiwavelength value to 1.8. The average mass concentration of PM_{10} for the rural background site before the dust plume occurred over SACOL and during the dust plume varied within a rather narrow range. The APS measurements showed a large number distribution (0.5–1 um particles) at SACOL during 2:00–8:00 (LST), which was higher than 10 #/cm3. The number concentration of PM_{10} increased gradually within the range 0.5–1 um, peaked at 15 #/cm3, and then decreased to > 1 um at SACOL during the non dust plume period. At Zhangye, the number concentration decreased gradually in the range of 0.5–10 um. The diameter (Dp) of PM_{10} was larger in the dust plume period than in the non dust plume period. During the dust plume period, the fine mode particles decreased, as did large-sized particles. This indicated that local floating dust occurred at that time.

[24] This study confirmed that the dust plume was transported from the remote desert regions over long distances. Furthermore, the stations are closed to desert, so local dust emission should also contribute to the observation and local air pollutants had a large influence on air quality in the regions need to further discuss. Dust storms may be contributed to the desertification of the Northwest China during recent decades. The results presented here represent only a first step in better understanding the effect of Asian dust on its optical and physical properties. Further research should be focused on measurements of the processes of local air pollutants.

[25] **Acknowledgments.** This research is supported by the National Satellite Meteorological Center, CMA under grant 2008BAC40B05–02, and the Fundamental Research Funds for the Central Universities under grant 860034. The OMI AI image and data used in this study were acquired using OMI flown on the EOS Aura spacecraft. The authors also gratefully acknowledge the NOAA Air Resources Laboratory for the provision of the HYSPLIT transport and dispersion model and/or READY Web site (http://www.arl.noaa.gov/ready.html) and the AOD data from AERONET Web site (http://aeronet.gsfc.nasa.gov) used in this publication. We are grateful to R. Coulter of the Argonne National Lab for loaning a MPL used in this study. We are grateful to all people that participated in the field experiment in Semi-Arid Climate and Environment Observatory of Lanzhou University (SACOL).

References

Ahmad, S. P., P. F. Levelt, P. K. Bhartia, E. Hilsenrath, G. W. Leppelmeier, and J. E. Johnson (2003), Atmospheric products from the ozone monitoring instrument (OMI), in *Earth Observing Systems VIII*, edited by W. L. Barnes, vol. 5151, pp. 619–630, Soc. of Photo-Opt. Instrum. Eng., San Diego, Calif.

Anderson, T. L., and J. A. Ogren (1998), Determining aerosol radiative properties using the TSI 3563 integrating nephelometer, *Aerosol Sci. Technol.*, *29*(1), 57–69, doi:10.1080/02786829808965551.

Anderson, T. L., et al. (1996), Performance characteristics of a high-sensitivity, three-wavelength, total scatter/backscatter nephelometer, *J. Atmos. Oceanic Technol.*, *13*, 967–986.

Arimoto, R., X. Y. Zhang, B. J. Huebert, C. H. Kang, D. L. Savoie, J. M. Prospero, S. K. Sage, C. A. Schloesslin, H. M. Khaing, and S. N. Oh (2004), Chemical composition of atmospheric aerosols from Zhenbeitai China, and Gosan, South Korea, during ACE-Asia, *J. Geophys. Res.*, *109*, D19S04, doi:10.1029/2003JD004323.

Brock, C. A., et al. (2004), Particle characteristics following cloud-modified transport from Asia to North America, *J. Geophys. Res.*, *109*, D23S26, doi:10.1029/2003JD004198.

Conant, W. C., J. H. Seinfeld, J. Wang, G. R. Carmichael, Y. Tang, I. Uno, P. J. Flatau, K. M. Markowicz, and P. K. Quinn (2003), A model for the radiative forcing during ACE-Asia derived from CIRPAS Twin Otter and R/V Ronald H. Brown data and comparison with observations, *J. Geophys. Res.*, *108*(D23), 8661, doi:10.1029/2002JD003260.

Corrigan, C. E., V. Ramanathan, and J. J. Schauer (2006), Impact of monsoon transitions on the physical and optical properties of aerosols, *J. Geophys. Res.*, *111*, D18208, doi:10.1029/2005JD006370.

Chung, C. E., V. Ramanathan, and J. T. Kiehl (2002), Effects of the south Asian absorbing haze on the northeast monsoon and surface-air heat exchange, *J. Clim.*, *15*(17), 2462–2476.

de Gouw, J. A., et al. (2004), Chemical composition of air masses transported from Asia to the U. S. West Coast during ITCT 2K2: Fossil fuel combustion versus biomass-burning signatures, *J. Geophys. Res.*, *109*, D23S20, doi:10.1029/2003JD004202.

Dickerson, R. R., M. O. Andreae, T. Campos, O. L. Mayol-Bracero, C. Neusuess, and D. G. Streets (2002), Analysis of black carbon and carbon monoxide observed over the Indian Ocean: Implications for emissions and photochemistry, *J. Geophys. Res.*, *107*(D19), 8017, doi:10.1029/2001JD000501.

Ding, R., J. Li, S. Wang, and F. Ren (2005), Decadal change of the spring dust storm in northwest China and the associated atmospheric circulation, *Geophys. Res. Lett.*, *32*, L02808, doi:10.1029/2004GL021561.

Draxler, R. R., and G. D. Hess (1998), An overview of the HYSPLIT_4 modelling system for trajectories, dispersion and deposition, *Aust. Meteorol. Mag.*, *47*(4), 295–308.

Duncan, B. N., R. V. Martin, A. C. Staudt, R. Yevich, and J. A. Logan (2003), Interannual and seasonal variability of biomass burning emissions constrained by satellite observations, *J. Geophys. Res.*, *108*(D2), 4100, doi:10.1029/2002JD002378.

Eldering, A., J. A. Ogren, Z. Chowdhury, L. S. Hughes, and G. R. Cass (2002), Aerosol optical properties during INDOEX based on measured aerosol particle size and composition, *J. Geophys. Res.*, *107*(D22), 8001, doi:10.1029/2001JD001572.

Fialho, F. A. P., L. P. Travasso, and M. Carvalho (2005), Multiple intelligence imagetic scenarios for leadership vision communication, paper presented at Fourth International Cyberspace Conference on Ergonomics, Int. Erg. Assoc., Johannesburg, South Africa.

Ge, J. M., J. Su, T. P. Ackerman, Q. Fu, J. P. Huang, and J. S. Shi (2010), Dust aerosol optical properties retrieval and radiative forcing over northwestern China during the 2008 China-U.S. joint field experiment, *J. Geophys. Res.*, *115*, D00K12, doi:10.1029/2009JD013263.

Gong, S. L., X. Y. Zhang, T. L. Zhao, I. G. Mckendry, D. A. Jaffe, and N. M. Lu (2003), Characterization of soil dust aerosol in China and its transport and distribution during 2001 ACE-Asia: 2. Model simulation and validation, *J. Geophys. Res.*, *108*(D9), 4262, doi:10.1029/2002JD002633.

Gong, S. L., X. Y. Zhang, T. L. Zhao, and L. A. Barrie (2004), Sensitivity of Asian dust storm to natural and anthropogenic factors, *Geophys. Res. Lett.*, *31*, L07210, doi:10.1029/2004GL019502.

Gu, Y., K. N. Liou, W. Chen, and H. Liao (2010), Direct climate effect of black carbon in China and its impact on dust storms, *J. Geophys. Res.*, *115*, D00K14, doi:10.1029/2009JD013427.

Heald, C. L., D. J. Jacob, R. J. Park, L. M. Russell, B. J. Huebert, J. H. Seinfeld, H. Liao, and R. J. Weber (2005), A large organic aerosol source in the free troposphere missing from current models, *Geophys. Res. Lett.*, *32*, L18809, doi:10.1029/2005GL023831.

Holben, B. N., et al. (1998), AERONET–A federated instrument network and data archive for aerosol characterization, *Remote Sens. Environ.*, *66*, 1–16, doi:10.1016/S0034-4257(98)00031-5.

Huang, J. P., P. Minnis, B. Lin, T. Wang, Y. Yi, Y. Hu, S. Sun-Mack, and K. Ayers (2006a), Possible influences of Asian dust aerosols on cloud properties and radiative forcing observed from MODIS and CERES, *Geophys. Res. Lett.*, *33*, L06824, doi:10.1029/2005GL024724.

Huang, J. P., B. Lin, P. Minnis, T. Wang, X. Wang, Y. Hu, Y. Yi, and J. K. Ayers (2006b), Satellite-based assessment of possible dust aerosols semi-direct effect on cloud water path over East Asia, *Geophys. Res. Lett.*, *33*, L19802, doi:10.1029/2006GL026561.

Huang, J. P., P. Minnis, Y. H. Yi, Q. Tang, X. Wang, Y. X. Hu, Z. Y. Liu, K. Ayers, C. Trepte, and D. Winker (2007), Summer dust aerosols detected from CALIPSO over the Tibetan Plateau, *Geophys. Res. Lett.*, *34*, L18805, doi:10.1029/2007GL029938.

Huang, J. P., P. Minnis, B. Chen, Z. Huang, Z. Liu, Q. Zhao, Y. Yi, and J. K. Ayers (2008a), Long-range transport and vertical structure of Asian dust from CALIPSO and surface measurements during PACDEX, *J. Geophys. Res.*, *113*, D23212, doi:10.1029/2008JD010620.

Huang, J. P., et al. (2008b), An overview of the Semi-Arid Climate and Environment Research Observatory over the Loess Plateau, *Adv. Atmos. Sci.*, *25*(6), 906–921, doi:10.1007/s00376-008-0906-7.

Huang, Z., J. Huang, J. Bi, G. Wang, W. Wang, Q. Fu, Z. Li, S.-C. Tsay, and J. Shi (2010), Dust aerosol vertical structure measurements using three MPL lidars during 2008 China-U.S. joint dust field experiment, *J. Geophys. Res.*, *115*, D00K15, doi:10.1029/2009JD013273.

Huebert, B. J., T. Bates, P. B. Russsell, G. Shi, Y. J. Kim, K. Kawamura, G. Carmichael, and T. Nakajima (2003), An overview of ACE-Asia: Strategies for quantifying the relationships between Asian aerosols and their climatic impacts, *J. Geophys. Res.*, *108*(D23), 8633, doi:10.1029/2003JD003550.

Husar, R. B., et al. (2001), Asian dust events of April 1998, *J. Geophys. Res.*, *106*, 18,317–18,330, doi:10.1029/2000JD900788.

Jaffe, D. A., et al. (1999), Transport of Asian air pollution to North America, *Geophys. Res. Lett.*, *26*, 711–714, doi:10.1029/1999GL900100.

Jaffe, D. A., S. Tamura, and J. Harris (2005), Seasonal cycle and composition of background fine particles along the west coast of the US, *Atmos. Environ.*, *39*, 297–306, doi:10.1016/j.atmosenv.2004.09.016.

Kim, S., A. Jefferson, S. Yoon, E. G. Dutton, J. A. Ogren, F. P. J. Valero, J. Kim, and B. N. Holben (2005), Comparisons of aerosol optical depth and surface shortwave irradiance and their effect on the aerosol surface radiative forcing estimation, *J. Geophys. Res.*, *110*, D07204, doi:10.1029/2004JD004989.

Lee, K. H., Z. Li, M. C. Cribb, J. Liu, L. Wang, Y. Zheng, X. Xia, H. Chen, and B. Li (2010), Aerosol optical depth measurements in eastern China and a new calibration method, *J. Geophys. Res.*, *115*, D00K11, doi:10.1029/2009JD012812.

Lelieveld, J., et al. (2001), The Indian Ocean experiment: Widespread air pollution from South and Southeast Asia, *Science*, *291*(5506), 1031–1036, doi:10.1126/science.1057103.

Li, C., L. T. Marufu, R. R. Dickerson, Z. Li, T. Wen, Y. Wang, P. Wang, H. Chen, and J. W. Stehr (2007), In-situ measurements of trace gases and aerosol optical properties at a rural site in northern China during EAST-AIRE IOP 2005, *J. Geophys. Res.*, *112*, D22S04, doi:10.1029/2006JD007592.

Li, C., et al. (2010), Anthropogenic air pollution observed near dust source regions in northwestern China during springtime 2008, *J. Geophys. Res.*, *115*, D00K22, doi:10.1029/2009JD013659.

Li, Z. (2004), Aerosol and climate: A perspective from east Asia, in *Observation, Theory, and Modeling of the Atmospheric Variability*, pp. 501–525, World Sci, Hackensack, N. J., doi:10.1142/9789812791139_0025.

Li, Z., et al. (2006), Aerosol optical properties and its radiative effects in northern China, *J. Geophys. Res.*, *112*, D22S01, doi:10.1029/2006JD007382.

Li, Z., et al. (2007a), Preface to special section on East Asian Studies of Tropospheric Aerosols: An International Regional Experiment (EAST-AIRE), *J. Geophys. Res.*, *112*, D22S00, doi:10.1029/2007JD008853.

Li, Z., et al. (2007b), Validation and understanding of Moderate Resolution Imaging Spectroradiometer aerosol products (C5) using ground-based measurements from the handheld Sun photometer network in China, *J. Geophys. Res.*, *112*, D22S07, doi:10.1029/2007JD008479.

Li, Z., et al. (2007c), Remote sensing of aerosol optical properties and its radiative effects in northern China, *J. Geophys. Res.*, *112*, D22S01, doi:10.1029/2006JD007382.

Littmann, T. (1991), Dust storm frequency in Asia: Cliamate control and variability, *Int. J. Climatol.*, *11*, 393–412, doi:10.1002/joc.3370110405.

Liu, D., Z. Wang, Z. Liu, D. Winker, and C. Trepte (2008), A height resolved global view of dust aerosols from the first year CALIPSO lidar measurements, *J. Geophys. Res.*, *113*, D16214, doi:10.1029/2007JD009776.

Liu, Z., et al. (2008), CALIPSO lidar observations of optical properties of Saharan dust: A case study of long-range transport, *J. Geophys. Res.*, *113*, D07207, doi:10.1029/2007JD008878.

Menon, S., J. Hansen, L. Nazarenko, and Y. F. Luo (2002), Climate effects of black carbon aerosols in China and India, *Science*, *297*(5590), 2250–2253, doi:10.1126/science.1075159.

Murayama, T., et al. (2001), Ground-based network observation of Asian dust events of April 1998 in East Asia, *J. Geophys. Res.*, *106*(D16), 18,345–18,359, doi:10.1029/2000JD900554.

Nakajima, T., et al. (2003), Significance of direct and indirect radiative forcings of aerosols in the East China Sea region, *J. Geophys. Res.*, *108*(D23), 8658, doi:10.1029/2002JD003261.

Prospero, J. M. (1996), Saharan dust transport over the North Atlantic Ocean and Mediterranean: An overview, in *The Impact of Desert Dust Across the Mediterranean*, edited by S. Guerzoni and R. Chester, Kluwer Acad., Dordrecht, Netherlands.

Prospero, J. M. (1999), Long-term measurements of the transport of African mineral dust to the southeastern United States: Implications for regional air quality, *J. Geophys. Res.*, *104*, 15,917–15,927, doi:10.1029/1999JD900072.

Qian, Y., D. Gong, J. Fan, L. R. Leung, R. Bennartz, D. Chen, and W. Wang (2009), Heavy pollution suppresses light rain in China: Observations and modeling, *J. Geophys. Res.*, *114*, D00K02, doi:10.1029/2008JD011575.

Ramanathan, V., et al. (2001), Indian Ocean experiment: An integrated analysis of the climate forcing and effects of the great Indo-Asian haze, *J. Geophys. Res.*, *106*(D22), 28,371–28,398, doi:10.1029/2001JD900133.

Ramanathan, V., C. Chung, D. Kim, T. Bettge, L. Buja, J. T. Kiehl, W. M. Washington, Q. Fu, D. R. Sikka, and M. Wild (2005), Atmospheric brown clouds: Impacts on south Asian climate and hydrological cycle, *Proc. Natl. Acad. Sci. U. S. A.*, *102*(15), 5326–5333, doi:10.1073/pnas.0500656102.

Streets, D. G., et al. (2001), Black carbon emissions in China, *Atmos. Environ.*, *35*, 4281–4296, doi:10.1016/S1352-2310(01)00179-0.

Sun, J., M. Zhang, and T. Liu (2001), Spatial and temporal characteristics of dust storms in China and its surrounding regions, 1960–1999: Relations to source area and climate, *J. Geophys. Res.*, *106*(D10), 10,325–10,333, doi:10.1029/2000JD900665.

Torres, O., P. K. Bhartia, J. R. Herman, Z. Ahmad, and J. Gleason (1998), Derivation of aerosol properties from satellite measurements of backscattered ultraviolet radiation: Theoretical basis, *J. Geophys. Res.*, *103*, 17,099–17,110, doi:10.1029/98JD00900.

VanCuren, R. A., and T. A. Cahill (2002), Asian aerosols in North America: Frequency and concentration of fine dust, *J. Geophys. Res.*, *107*(D24), 4804, doi:10.1029/2002JD002204.

VanCuren, R. A., S. S. Cliff, K. D. Perry, and M. Jimenez-Cruz (2005), Asian continental aerosol persistence above the marine boundary layer over the eastern North Pacific: Continuous aerosol measurements from Intercontinental Transport and Chemical Transformation 2002 (ITCT 2K2), *J. Geophys. Res.*, *110*, D09S90, doi:10.1029/2004JD004973.

Verma, S., O. Boucher, M. S. Reddy, S. K. Deb, H. C. Upadhyaya, P. Le Van, F. S. Binkowdki, and O. P. Sharma (2005), Tropospheric distribution of sulphate aerosol mass and number concentration during INDOEX-IFP and its transport over the Indian Ocean: A GCM study, *Atmos. Chem. Phys.*, *5*, 395–436, doi:10.5194/acpd-5-395-2005.

Wang, P., B. Wu, and W. Zhang (1999), Analysis on the factors affecting surface UV radiation, *Chin. J. Atmos. Sci.*, *1*, 1–8, doi:10.1007/BF02872044.

Wang, T., et al. (2004), Relationships of trace gases and aerosols and the emission characteristics at Lin'an, a rural site in eastern China, during spring 2001, *J. Geophys. Res.*, *109*, D19S05, doi:10.1029/2003JD004119.

Wang, X., J. P. Huang, M. X. Ji, and K. Higuchi (2008), Variability of East Asia dust events and their long-term trend, *Atmos. Environ.*, *42*, 3156–3165, doi:10.1016/j.atmosenv.2007.07.046.

Xia, X., H. Chen, and P. Wang (2004), Aerosol properties in a Chinese semiarid region, *Atmos. Environ.*, *25*(38), 4571–4581.

Xia, X. A., H. B. Chen, P. C. Wang, X. M. Zong, and P. Goloub (2005), Aerosol properties and their spatial and temporal variations over north China in spring 2001, *Tellus, Ser. B*, *57*, 28–39, doi:10.1111/j.1600-0889.2005.00126.x.

Xia, X., et al. (2006), Variation of column integrated aerosol properties in a Chinese urban region, *J. Geophys. Res.*, *111*, D05204, doi:10.1029/2005JD006203.

Xia, X., Z. Li, P. Wang, H. Chen, and M. Cribb (2007), Aerosol optical properties and radiative effects in the Yangtze Delta region of China, *J. Geophys. Res.*, *112*, D22S12, doi:10.1029/2007JD008859.

Zhang, M., et al. (2003), Large-scale structure of trace gas and aerosol distributions over the western Pacific Ocean during TRACE-P, *J. Geophys. Res.*, *108*(D21), 8820, doi:10.1029/2002JD002946.

Zhang, R. J., Y. F. Xu, and Z. W. Han (2003), Inorganic chemical composition and source signature of $PM_{2.5}$ in Beijing during ACE-Asia period, *Chin. Sci. Bull.*, *48*(10), 1002–1005.

Zhang, R. J., R. Arimoto, J. L. An, S. Yabuki, J. H. Sun (2005), Ground observation of a strong dust storm in Beijing in March 2002, *J. Geophys. Res.*, *110*, D18S06, doi:10.1029/2004JD004589.

Zhang, R. J., Z. Han, Z. Shen, and J. Cao (2008), Continuous measurement of number concentrations and elemental composition of aerosol particles for a dust storm event in Beijing, *Adv. Atmos. Sci.*, *25*(1), 89–95, doi:10.1007/s00376-008-0089-2.

Zhang, X. Y., R. Arimoto, and Z. S. An (1997), Dust emission from Chinese desert sources linked to variations in atmospheric circulation, *J. Geophys. Res.*, *102*(D23), 28,041–28,047, doi:10.1029/97JD02300.

Zhang, Y., Q. Yu, W. Ma, and L. Chen (2010), Atmospheric deposition of inorganic nitrogen to the eastern China seas and its implication to marine biogeochemistry, *J. Geophys. Res.*, *115*, D00K10, doi:10.1029/2009JD012814.

Zhou, Z. J., and X. W. Wang (2002), Analysis of the severe group dust storms in eastern part of northwest China, *J. Geogr. Sci.*, *12*, 357–362, doi:10.1007/BF02837557.

J. Bi, B. Chen, J. Huang, X. Wang, and R. Zhang, Key Laboratory for Semi-Arid Climate Change of the Ministry of Education, College of Atmospheric Sciences, Lanzhou University, Lanzhou, 730000, China. (wxin@lzu.edu.cn)